frontiers | Frontiers in Mechanical Engineering

TYPE Original Research
PUBLISHED 19 February 2025
DOI 10.3389/fmech.2025.1497939

OPEN ACCESS

EDITED BY
Dipankar Chatterjee,
Central Mechanical Engineering Research Institute (CSIR), India

REVIEWED BY
Titan C. Paul,
University of South Carolina Aiken, United States
Abhiram Hens,
National Institute of Technology, Durgapur, India

*CORRESPONDENCE
Gang Wang,
wanggang5288@163.com

RECEIVED 20 September 2024
ACCEPTED 28 January 2025
PUBLISHED 19 February 2025

CITATION
Zhang L, Yang H, Wang G and Wang Z (2025) Molecular dynamics simulation on the heat transfer at liquid-solid interfaces and enhancement mechanism.
Front. Mech. Eng. 11:1497939.
doi: 10.3389/fmech.2025.1497939

COPYRIGHT
© 2025 Zhang, Yang, Wang and Wang. This is an open-access article distributed under the terms of the Creative Commons Attribution License (CC BY). The use, distribution or reproduction in other forums is permitted, provided the original author(s) and the copyright owner(s) are credited and that the original publication in this journal is cited, in accordance with accepted academic practice. No use, distribution or reproduction is permitted which does not comply with these terms.

Molecular dynamics simulation on the heat transfer at liquid-solid interfaces and enhancement mechanism

Lihui Zhang[1], Huichuang Yang[1], Gang Wang[2]* and Zhongxu Wang[2]

[1]Department of Mechanical and Electrical Engineering, University of Shaoxing, Shaoxing, China, [2]School of Energy and Power Engineering, Northeast Electric Power University, Jilin, China

To investigate the effect of surface roughness on the heat transfer mechanism, a molecular dynamics model of heat transfer between solid and liquid interfaces was established in this paper. The temperature distribution, heat flux, thermal resistance, and number density distribution of water molecules in the interface are calculated and discussed systematically. The effects of energy parameters between solid and liquid, and the roughness level of the wall on the heat transfer performance were analyzed. The results show that as the energy parameter rises from 0.413 to 1.651 kcal/mol, the heat flux increases from 1.5×10^9 to 3.2×10^9 Wm^{-2}, and the thermal resistance at the cold and hot ends of the solid-liquid interface demonstrates a decreasing trend from 18.75×10^{-9} to 2.50×10^{-9} $Km^2 \cdot W^{-1}$. It indicates that the interaction between solid and liquid is enhanced, and more water molecules gather near the solid-liquid interface, which promotes energy transfer and thus strengthens the heat transfer between solid and liquid. As the depth of surface roughness varies from 1a to 2.5a, the static contact angle of droplets decreases from $69.06^\circ \pm 0.28^\circ$ to $49.98^\circ \pm 0.44^\circ$, slightly enhancing the hydrophilicity of the rough wall structure. Thus, compared with the smooth wall, the rough wall structure enables more water molecules to come into contact with the wall, thereby increasing the heat transfer area and consequently enhancing the heat flux and reducing the thermal resistance. With the increase of wall roughness, the cold (hot) thermal resistance further decreases from 19.2 (19.7) $\times 10^{-9}$ to 4.9 (5.0) $\times 10^{-9}$ $Km^2 \cdot W^{-1}$.

KEYWORDS

molecular dynamics, solid-liquid interface, thermal resistance, heat transfer, roughness

1 Introduction

Heat transfer is a process of spontaneous heat exchange caused by temperature difference (Li and Liu, 2012; Zhang et al., 2022). When the heat flow passes through the solid-liquid interface, there will be a temperature step, which is caused by the interfacial thermal resistance between solid and liquid (Chen and Zhang, 2014; Song L. et al., 2022). To achieve the goal of carbon peaking and carbon neutrality, apart from the development and utilization of new energy, enhancing the comprehensive utilization efficiency of energy and adopting certain measures for the efficient recycling of industrial waste heat is also a highly significant approach. In the industrial waste heat recovery system, the heat exchanger is the core equipment. The heat transfer characteristics at the solid-liquid interface also have an

impact on the efficiency of waste heat recovery and utilization. Therefore, strengthening the heat transfer at the solid-liquid interface is an effective way to enhance the efficiency of the waste heat recovery and utilization. Besides, with the progress of science and technology, the performance of computers and other electronic equipments have been significantly improved, which has brought great convenience to our lives and scientific research work. However, the electronic equipment will generate a lot of heat during its operation, which results in high temperature, and heat flux concentration of micro- and nano-electronic components, seriously affecting its service life. Therefore, it puts forward higher requirements for enhancing heat transfer at the micro and nano scale (Su et al., 2024; Warzoha et al., 2021).

It is proved that changing the structural characteristics of the surface is an important method to enhance the heat transfer characteristics at the solid-liquid interface (Yin et al., 2019a; Cao and Cui, 2019; Liu et al., 2020), which is widely used in the heat dissipation of micro and nano components (Liu et al., 2019; Sun et al., 2020). The experimental system for microscale heat transfer at the solid-liquid interfaces is complex and expensive to construct. With the development of computers, molecular simulation methods can be used to overcome such difficulties. In recent years, many researchers have adopted molecular dynamics methods to simulate the heat transfer process between solid and liquid interfaces (Qian et al., 2024; Sun et al., 2024; Zhou et al., 2024). In micro/nano scale, there would be an obvious temperature slip at the solid-liquid interface, and the decrease in wettability of the interface would lead to an increase in the thermal resistance (Liu et al., 2024). Kim et al. (2008) proposed a hot wall model based on the actual situation, which simulated the heat exchange process between liquid and solid walls. It was found that when the interaction between liquid and solid surfaces is strong, no temperature slip phenomenon appears at the interface. However, if the interaction is weak or the solid wall is hard, there will be a significant temperature slip at the solid-liquid interface. It indicates that the existence of this temperature slip is related to the strength of the liquid-solid interaction and is also affected by the stiffness of the solid wall. He et al. (2011) used the non-equilibrium molecular dynamics method to investigate the heat transfer phenomenon at the rough solid-liquid interface at the nanoscale and analyzed the influence of the wettability of the wall surface on the heat transfer at the solid-liquid interface. Tang et al. (2021) took ionic liquid as the research object and established a molecular heat transfer model at the interface between electrodes and electrolytes. Their results show that when the electrode is charged, a stable double-layer charge structure is formed near the electrode, which increases the heat transfer efficiency at the interface. Li et al. (2022) found that increasing the interface coupling strength or placing nanostructures on the solid interface could enhance the interface heat transfer.

There has been some research on heat transfer at solid-liquid interfaces analyzing the effects of interfacial forces, wall wettability, temperature gradients, surface roughness and other factors on the heat transfer at solid-liquid interfaces. Especially for the studies on the effect of rough wall surfaces on the heat transfer characteristics of the solid-liquid interface, most of the studies model the walls with simple zigzag, rectangular or trapezoidal shapes, where the structure of the rough wall exists in the form of a bump. However, there are few reports related to the research of rough walls with the structure of both convex and concave shapes. Aims to reveal the influence of the depth of convex and concave structures on heat transfer at the solid-liquid interface, in this paper, the shape of the interface is selected with a structure similar to the sine curve distribution, and molecular dynamics method was applied to simulate the heat transfer process between solid and liquid. And the influence of surface wettability and the depth of wall roughness on the heat transfer process at the solid-liquid interface were investigated. The temperature distribution, heat flux, solid-liquid thermal resistance, and number density profiles of water molecules under different working conditions were also calculated to reveal the heat transfer enhancement mechanisms.

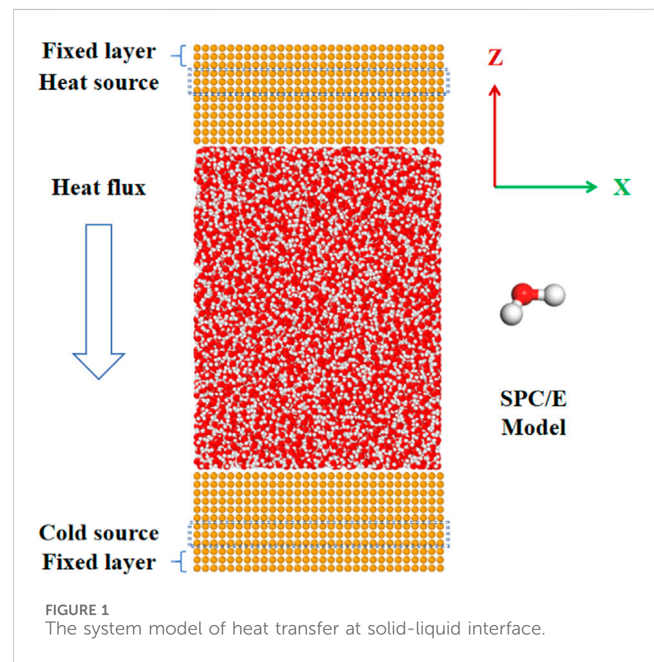

FIGURE 1
The system model of heat transfer at solid-liquid interface.

2 Model and simulation method

2.1 Model

The system diagram of heat transfer simulation at the solid-liquid interface is shown in Figure 1. The whole heat transfer system consists of two parts: solid and liquid regions. The solid wall is composed of a certain number of copper atoms arranged in face-centered cubic (FCC) form, and the lattice constant of copper atom is set as a = 3.55212 Å. The copper walls at top and bottom sides of the system have the same size of 53.2818 Å (=15a) along both the x and y directions. In order to maintain the stability of the system, two fixed atomic layers with a length of a are arranged at both ends of the solid wall. Next to the fixed layers, three layers of copper atoms are defined as the heat and cold source regions respectively along z direction, which can drive the system to generate heat flow. The thickness of the cold and heat source region is a. The rest of the solid area is the heat transfer layer.

In order to explore the influence of rough structure on the interfacial heat transfer, four kinds of rough surfaces were constructed. Taking the rough solid wall marked H1.5a in

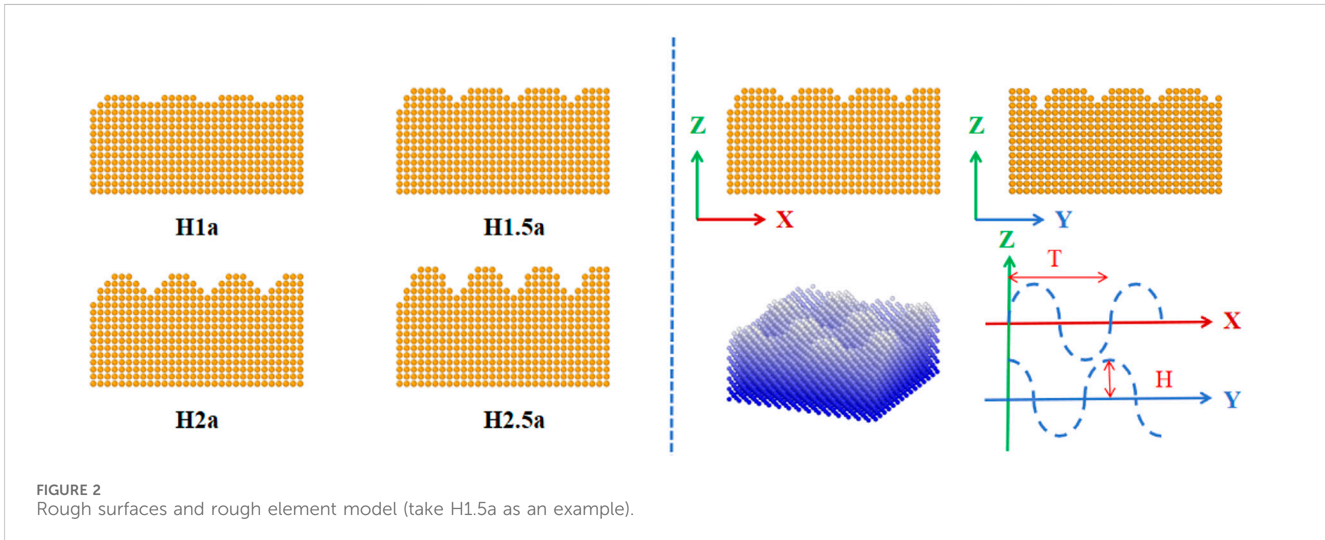

FIGURE 2
Rough surfaces and rough element model (take H1.5a as an example).

TABLE 1 The interaction parameters of each atom in the potential function.

Atom	σ/Å	ε/kcal·mol^{-1}	q/e
O	3.166	0.1553	−0.8476
H	0	0	0.4238
Cu	2.277	9.8686	0

Figure 2 as an example, the construction method of the rough solid walls is described as follows. The surface of rough wall presents a regular convex and convex structure, that is, the distribution of rough elements along the x and y direction follows sine and cosine law respectively, and the fluctuation height of the rough structure is equal to the depression depth. The length of change period is held constant to be T (T = 8a) for both x and y directions, where a is the lattice constant of copper atom, a = 3.552 Å. Four kinds of rough wall surfaces, marked as H1a, H1.5a, H2a and H2.5a in Figure 2, can be obtained by changing the height of rough element to be a, 1.5a, 2a and 2.5a respectively. It is noted that the amplitudes of convex and concave structure are equal for one specified roughness.

The liquid region is composed of 6,700 water molecules, and the SPC/E model is used to describe the movement of water molecules, which has been successfully applied in the research of wetting and heat transfer of droplets (Song et al., 2020). The Shake algorithm is used to fix the bond length and bond angle of water molecules. For SPC/E model of water molecules, the length of hydrogen/oxygen bond is 0.10 nm and the angle of bond is 109.47°. The interaction potential function between water molecules is determined by:

$$U(r_{ij}) = \frac{1}{4\pi\varepsilon_0}\sum_{i=1}^{3}\sum_{j=1}^{3}\frac{q_i q_j}{r_{ij}} + 4\varepsilon_{oo}\left[\left(\frac{\sigma_{oo}}{r_{ij}}\right)^{12} - \left(\frac{\sigma_{oo}}{r_{ij}}\right)^{6}\right] \tag{1}$$

In Equation 1, the first term calculates the coulomb force between charged atoms, where q_i and q_j are the charge quantity of atom i and j respectively, r_{ij} represents the distance between atoms i and j, and ε_0 is the vacuum dielectric constant; The second term is the potential energy and is used to calculate the short-range van der Waals forces that exist between oxygen atoms. The effect of force generated by hydrogen atoms is ignored due to their small mass. σ_{oo} and ε_{oo} represent the scale and energy parameters of the interaction between oxygen atoms, respectively. Table 1 shows the interaction parameters of each atom in the potential function.

The interaction between the oxygen atom of the water molecule and the copper atom of the wall is characterized by the modified L-J potential function as shown in Equation 2:

$$U_{cu-o}(r_{ij}) = 4_{\varepsilon cu-o}\left[\left(\frac{\sigma_{cu-o}}{r_{ij}}\right)^{12} - \left(\frac{\sigma_{cu-o}}{r_{ij}}\right)^{6}\right] \tag{2}$$

where the parameters σ_{cu-o} and ε_{cu-o} are calculated by Lorentz-Bertholet mixed rules (Song et al., 2023) according to Equations 3, 4:

$$\sigma_{cu-o} = \frac{\sigma_{cu} + \sigma_o}{2} \tag{3}$$

$$\varepsilon_{cu-o} = \sqrt{\varepsilon_{cu}\varepsilon_o} \tag{4}$$

2.2 Simulation method

In this paper, the simulation of molecular dynamics was calculated by LAMMPS software (Boone et al., 2019; Song et al., 2025). Periodic boundary conditions are applied in all three directions xyz. In the z direction, the presence of upper and lower copper walls has a binding effect on the internal water molecules, and the internal water molecules will not cross the copper walls. Therefore, taking periodic boundary conditions in the z direction doesn't affect the heat transfer. The Velocity-Verlet algorithm is used to solve the Newton equation, and the time step is 1 fs. The truncation radius employed for calculating the interaction of LJ and Coulomb is 1.5 nm, where the long-range electrostatic force is modified by the PPPM method. In the simulation, the whole process of heat transfer is divided into three stages: relaxation equilibrium, heat transfer, and data acquisition. In the relaxation equilibrium process, the NVT ensemble and Nose-Hoover thermostat (Liu et al., 2021) were used to control the temperature of the whole system at 300 K. The system was fully relaxed and reached equilibrium during the simulation time of 1 ns.

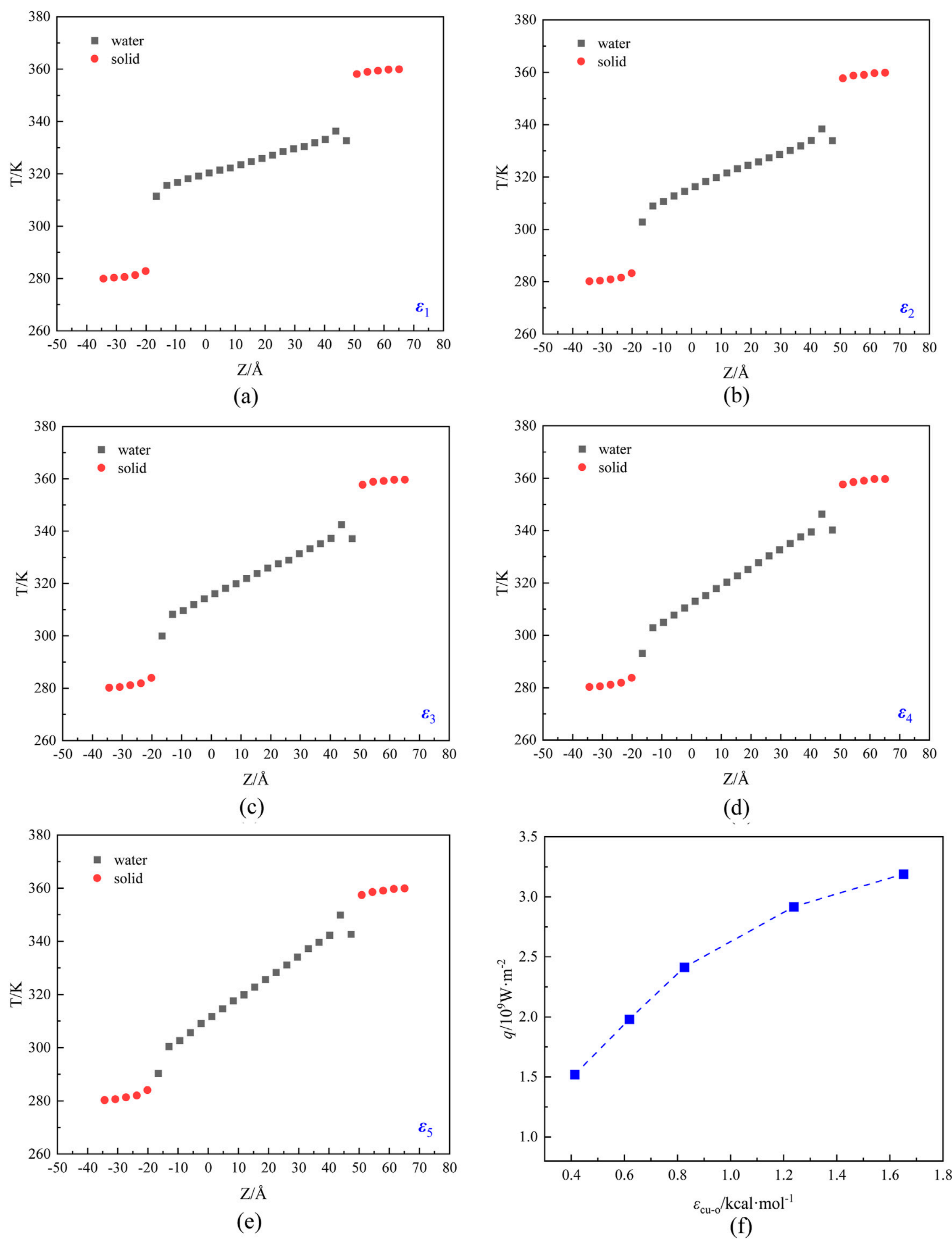

FIGURE 3
The temperature and heat flux distribution of the system under different solid-liquid energy parameters: **(A)** ε_1 = 0.413, **(B)** ε_2 = 0.619, **(C)** ε_3 = 0.826, **(D)** ε_4 = 1.238, **(E)** ε_5 = 1.651, and **(F)** heat flux.

In the heat transfer process, the simulation system was set to be NVE ensemble. Langevin temperature control (Yin et al., 2019b) is used to control the temperature of cold and hot source regions at 280 and 360 K, respectively. The simulation time for this process is 4 ns. In the data collection process, atomic information is output and stored every 1,000 steps. The particle information is averaged every 200,000 steps in order to obtain the parameters of temperature, heat flux, and thermal resistance at the solid-liquid interface.

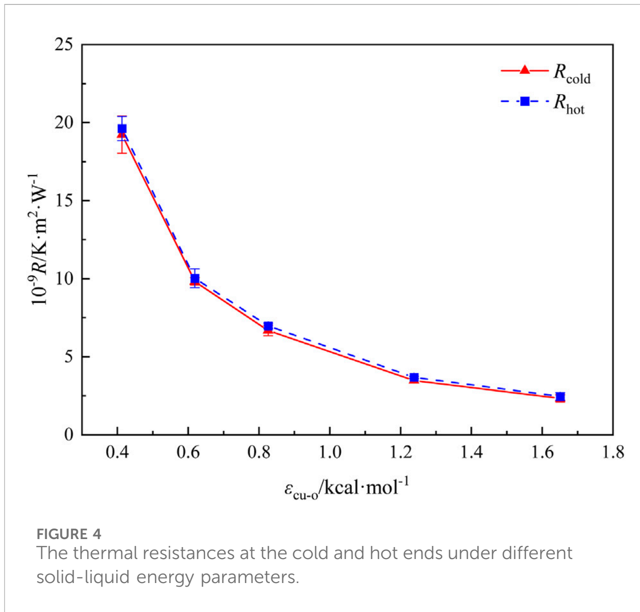

FIGURE 4
The thermal resistances at the cold and hot ends under different solid-liquid energy parameters.

The heat flux along the heat transfer direction can be calculated according to Equation 5, Wu et al. (2020):

$$q = \frac{\Delta E}{2A\Delta t} \tag{5}$$

where A is the cross-sectional area perpendicular to the direction of heat transfer, Δt is the simulation time of heat transfer, and ΔE is the heat added or removed at each step by cold and hot sources. The thermal resistance at the solid-liquid interface can be calculated according to Equation 6, Qian et al. (2018), Yang and Cao (2024):

$$R = \frac{\Delta T}{q} \tag{6}$$

where ΔT is the temperature step at the solid-liquid interface, and q is the heat flux of heat transfer system. In this paper, the temperature of the cold and hot source area is set at 280 and 360 K respectively by trade-offs of accuracy and computational efficiency.

2.3 Validation

To validate this simulation model, we constructed a molecular dynamics model of nano water droplets wetting on a smooth copper solid wall, and an equilibrium contact angle was obtained based on the statistical analysis of droplet density distribution. It was found that the equilibrium contact angle of the droplet on the copper wall was approximately 76.48° ± 0.63°, which was in good accordance with the results in the literature (Hong et al., 1994).

3 Results and discussion

In order to ensure the rationality and accuracy of simulated heat transfer, it is noted that the temperature difference between the cold and hot source regions should be set reasonably to ensure that micro-nano droplets will not undergo phase change during the heat transfer process.

3.1 Effect of solid-liquid energy parameters on heat transfer

The solid wall in the solid-liquid interface heat transfer model is constructed with copper wall atomic configuration, in order to discuss the influence of different wettability walls on the solid-liquid interface heat transfer. The wettability of the solid wall can be determined by changing the energy parameters of the solid-liquid interface, which can simplify the model and save the simulation time. Therefore, $\varepsilon_1 = 0.413$, $\varepsilon_2 = 0.619$, $\varepsilon_3 = 0.826$, $\varepsilon_4 = 1.238$ and $\varepsilon_5 = 1.651$ kcal/mol are selected to represent the five kinds of wall surfaces with different wettability. Obviously, the wettability of the surface assigned with a larger energy parameter(ε) is better than the surface assigned with a smaller ε.

At the beginning of simulation, driven by the temperature difference, the micro and nano droplets carried out the heat absorption and release process on the cold and hot wall respectively, which gradually approaches the steady state. When

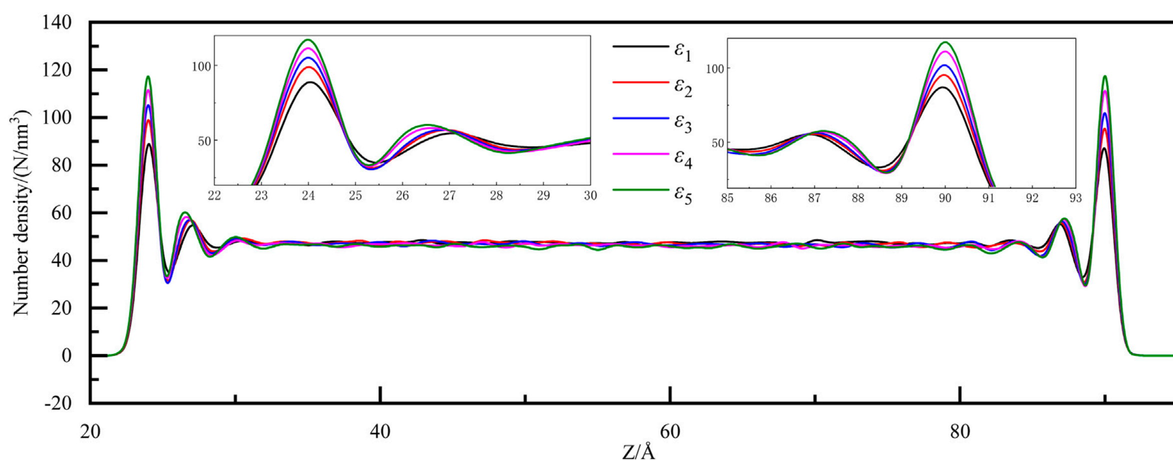

FIGURE 5
The number density distribution of water molecules along the heat transfer direction under different solid-liquid energy parameters.

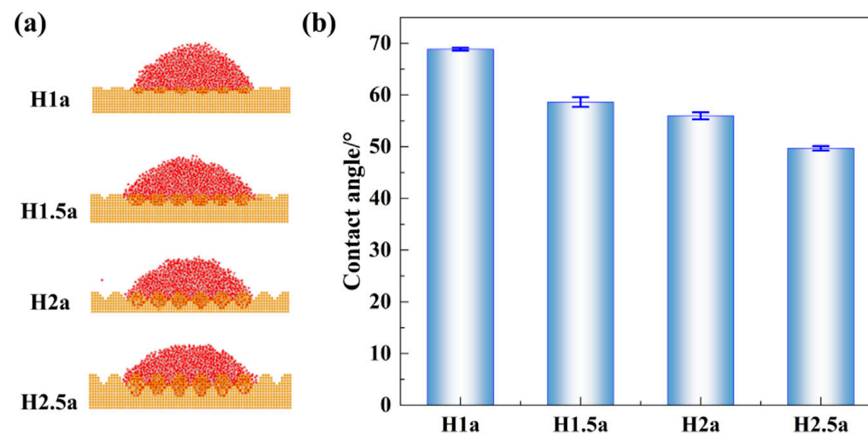

FIGURE 6
(A) Simulation snapshots of equilibrium state of nano-water droplets wetting on different rough surfaces and (B) the corresponding static contact angles.

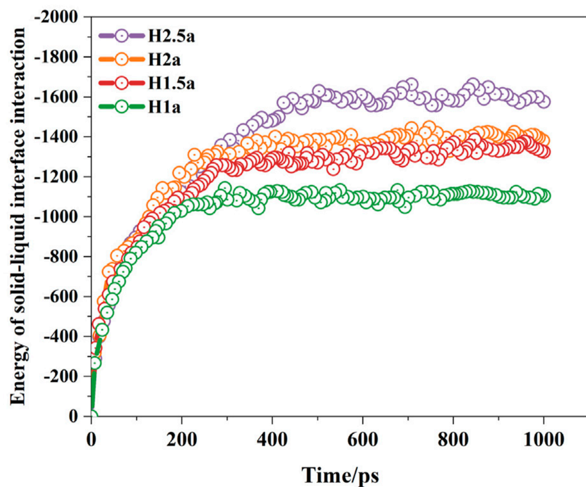

FIGURE 7
Variation of solid-liquid interaction energy of nano-droplets on different rough surfaces.

the heat transfer reaches equilibrium, the block average method (Song F. H. et al., 2022) is used to calculate the temperature distribution of the entire heat transfer system. Figure 3 shows the temperature distribution of the solid and liquid regions, together with the corresponding heat flux of the system.

As shown in Figures 3A–E, the slope of the temperature distribution in the liquid region is significantly greater than that on the solid wall, indicating that the thermal conductivity of the solid is much greater than that of the liquid. There is an obvious temperature discontinuity at the solid-liquid interface, that is, the temperature slip, which is due to the thermal resistance at the solid-liquid interface. When the energy parameters increases from ε_1 to ε_5, the temperature in the liquid region rises at a larger slope, and the temperature slip at the solid-liquid interface presents an obvious decreasing trend. The heat flux of the system is computed by Equation 5, and the outcomes are presented in Figure 3F. It can be observed that the heat flux rises when the energy parameter is increased, however, the increase is decreasing.

It can be seen that under different energy parameters, the temperature distribution of the heat transfer system conforms to the linear distribution law, so the Fourier thermal conductivity law can be used to calculate the thermal resistance at the solid-liquid interface. Based on the temperature slip and the corresponding heat flux depicted in Figure 3, the thermal resistance at the hot and cold ends of the solid-liquid interface can be computed by Equation 6. The results are shown in Figure 4. Obviously, the thermal resistance at the hot and cold ends tends to be equal, and as the solid-liquid energy parameter increases from 0.413 to 1.651 $\text{kcal}\cdot\text{mol}^{-1}$, the thermal resistance at the cold and hot ends of the solid-liquid interface shows a decreasing trend from 18.75×10^{-9} $\text{K}\cdot\text{m}^2\cdot\text{W}^{-1}$to 2.50×10^{-9} $\text{K}\cdot\text{m}^2\cdot\text{W}^{-1}$.

When the heat transfer attains a stable equilibrium, the number density distribution of water molecules along the heat transfer direction is also computed, as shown in Figure 5. In the middle of the system, the distribution of water molecules is relatively uniform and stable, while the peak emerges at the solid-liquid interfaces at both ends of the system. The reason for this phenomenon is that, attracted by the solid wall, a large number of water molecules gather near the solid-liquid interface. As the solid-liquid energy parameters increase, the force exerted by water molecules on solid walls intensifies, therefore, more and more water molecules accumulate near the solid-liquid interface. Meanwhile, it also reasonably explains the phenomenon of liquid temperature slip near the solid-liquid interface in Figure 2.

3.2 Effect of wall roughness on heat transfer

In order to investigate the effect of wall roughness on heat transfer, four different roughness levels were set on the solid walls at both ends of the heat transfer system, and the heat transfer simulations of liquid on smooth and four rough surfaces were carried out. The energy parameter between the copper atom of

 10.3389/fmech.2025.1497939

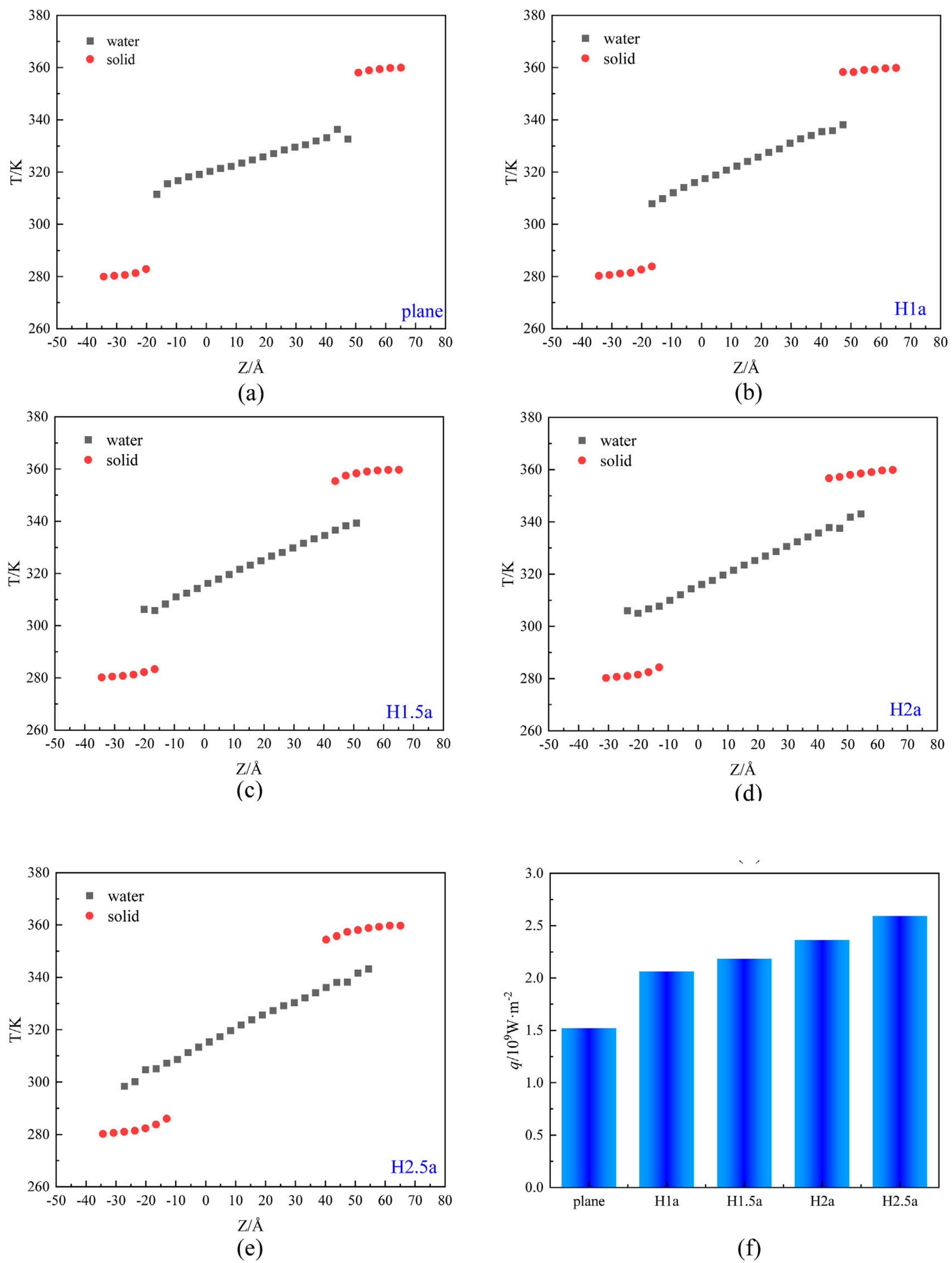

FIGURE 8
The steady-state temperature distribution **(A-E)** and heat flux **(F)** under different levels of wall roughness defined by the height of rough element, H (a) H=0 (plane), (b) H=a, (c) H=1.5a, (d) H=2a, (e) H=2.5a.

wall and the oxygen atom of the water molecule was set to be fixed, $\varepsilon_{cu\text{-}o}$ = 0.413 kcal/mol.

To explain the effect of surface roughness, it is important to make clear the relationship between the surface roughness and the surface wettability. The molecular dynamics models of nanodroplets wetting on different rough surfaces were constructed, and the static contact angle of the nanodroplets at equilibrium state was calculated according to the density counter, as discussed in our previous studies (Song F. H. et al., 2022), and then the influence of rough surface on heat transfer was further analyzed according to the changes in the wettability of rough walls. Figure 6 shows the simulated snapshot of the equilibrium state of nano-water droplets wetting on the rough

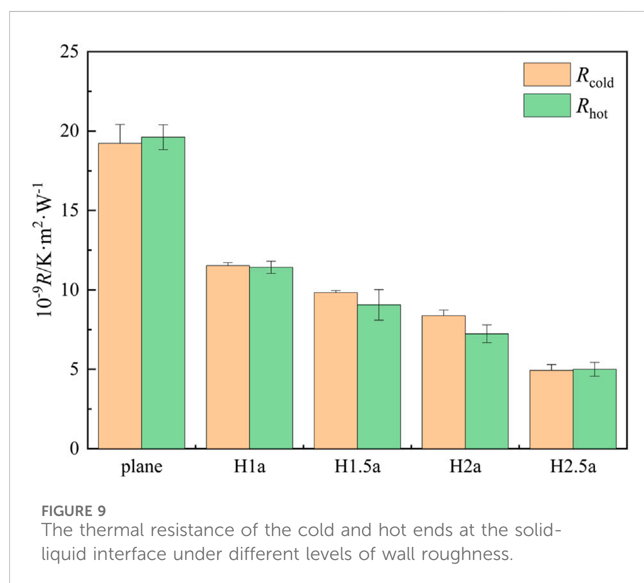

FIGURE 9
The thermal resistance of the cold and hot ends at the solid-liquid interface under different levels of wall roughness.

surface and the corresponding contact angles under different working conditions.

As can be seen from Figure 6, the droplets show different wetting states on surfaces with different roughness. Water molecules tend to accumulate in uneven areas due to the strong attraction of surface atoms. According to the distribution of the equilibrium wetting contact angle of nanodroplets on different rough surfaces, it can be seen that the static contact angle of droplets shows a decreasing trend with the increase of surface fluctuation and depression depth, that is, the hydrophilicity of the surface slightly increases with the increase of fluctuation and depression depth of rough surface. The corresponding contact angles are $69.06^{\circ} \pm 0.28^{\circ}$, $57.95^{\circ} \pm 0.93^{\circ}$, $56.44^{\circ} \pm 0.67^{\circ}$ and $49.98^{\circ} \pm 0.44^{\circ}$ for the roughness surfaces H1a, H1.5a, H2a, and H2.5a respectively.

Figure 7 shows the variation of solid-liquid interaction energy with time under different rough surface conditions. It can be seen that when the droplet contacts with the rough surface, the water molecules start to wet and spread under the interaction of the wall surface, and the wetting contact area increases, so does the solid-liquid interaction energy. The solid-liquid interaction energy tends to be stable when the droplet wetting reaches equilibrium. Moreover, when the depth of the rough surface increases, more water molecules enter the grooves on the surface, the actual contact area between the droplet and the solid surface becomes larger, and the solid-liquid interaction could be enhanced, which leads to a stronger attraction from the solid substrate, stronger hydrophilicity of the surface, and a decrease in the wetting contact angle.

For the heat transfer model, when the heat transfer process reaches a stable equilibrium, the temperature distribution and heat flux of the system are shown in Figure 8. From Figures 8A–E, it is observed that the slopes of the temperature distribution in the liquid region are very close since the same energy parameter is used. Compared to the result of heat transfer on a smooth copper wall (Figure 8A), the temperature distribution overlaps at the solid-liquid interface for rough walls (Figures 8B–E). The reason for this phenomenon is the existence of grooves on the rough walls. During the heat transfer process, some water molecules will enter the groove and form a liquid Mosaic configuration at the solid-liquid interface. As the depth of roughness surface increases, more water molecules enter the grooves, and result in the temperature overlap more obvious. In addition, it is also observed that the temperature slip at the solid-liquid interface is smaller on the rough wall compared to the smooth wall. The comparison of heat flux under different surface roughness is shown in Figure 8F. Clearly, the heat flux increases with the increase of surface roughness. This is because the rough wall surface is more hydrophilic compared to the smooth one and the surface wettability also become to be better as the increase of H, which makes the contact area between the droplet and wall larger, thus promoting the exchange of energy and enlarging the heat flux.

Based on the results of temperature and heat flux in Figure 8, the thermal resistance is calculated by Equation 6. The results of thermal resistance at the solid-liquid interface are shown in Figure 9. Similarly, for smooth and rough wall surfaces, the thermal resistance of the cold and hot end has no significant difference. When the heat is transferred on the rough wall surface, the thermal resistance at the hot and cold ends decreases significantly compared with the smooth wall surface, and the thermal resistance decreases further with the increase of wall roughness. For the wall roughness H-2.5a, the corresponding thermal resistance at the cold and hot ends are reduced by $13.5 \times 10^{-9}$and 14×10^{-9} K $\cdot$m^2·W^{-1}, respectively, compared to the smooth plane.

4 Conclusion

In this paper, the non-equilibrium molecular dynamics method is employed to simulate the interfacial heat transfer characteristics of water on a rough wall. The solid-liquid interaction can be represented by changing the energy parameters of solid-liquid interaction. As the energy parameters increase, more water molecules accumulate near the solid-liquid interface, resulting in the augmentation of heat flux from 1.5×10^9 to 3.2×10^9 W $\cdot$m^{-2}, and the reduction of the temperature slip and thermal resistance between the solid and the liquid. The effect of solid wall roughness on heat transfer is investigated. Compared with the smooth copper wall, the rough structure can expand the solid-liquid heat transfer area, enabling more water molecules in contact with the solid wall, thereby enhancing heat transfer. With the increase of wall roughness, the heat flux between the solid and the liquid rises, and the temperature slip and interfacial thermal resistance decline. Compare to the smooth wall surface, the thermal resistance at the cold and hot ends is reduced by 14.3×10^{-9} and 14.7×10^{-9} K $\cdot$m^2·W^{-1} when the depth of wall roughness is 2.5a. The research findings of this paper offer a novel perspective for enhancing the heat transfer at the solid-liquid interface, and lay a theoretical foundation for the development of micro-nano electronic device cooling technology and the field of waste heat recovery and utilition.

Data availability statement

The original contributions presented in the study are included in the article/supplementary material, further inquiries can be directed to the corresponding author.

Author contributions

LZ: Conceptualization, Data curation, Formal Analysis, Writing–original draft, Writing–review and editing. HY: Data curation, Formal Analysis, Writing–review and editing. GW: Conceptualization, Writing–review and editing. ZW: Software, Writing–original draft.

Funding

The author(s) declare that financial support was received for the research, authorship, and/or publication of this article. The authors acknowledge the financial support provided by Key Technology Research and Development Plan of Jilin Province (Grant No. 20240304098SF).

Conflict of interest

The authors declare that the research was conducted in the absence of any commercial or financial relationships that could be construed as a potential conflict of interest.

Publisher's note

All claims expressed in this article are solely those of the authors and do not necessarily represent those of their affiliated organizations, or those of the publisher, the editors and the reviewers. Any product that may be evaluated in this article, or claim that may be made by its manufacturer, is not guaranteed or endorsed by the publisher.

References

Boone, P., Babaei, H., and Wilmer, C. E. (2019). Heat flux for many body interactions: corrections to LAMMPS. *J. Chem. Theory Comput.* 15, 5579–5587. doi:10.1021/acs.jctc.9b00252

Cao, Q., and Cui, Z. (2019). Molecular dynamics simulations of the effect of surface wettability on nanoscale liquid film phase-change. *Numer. Heat. Tr. A-Appl* 75 (8), 533–547. doi:10.1080/10407782.2019.1608768

Chen, Y. P., and Zhang, C. B. (2014). Role of surface roughness on thermal conductance at liquid-solid interfaces. *Int. J. Heat. Mass Tran.* 78, 624–629. doi:10.1016/j.ijheatmasstransfer.2014.07.005

He, Y. L., Cao, W., Yin, X., and Yang, B. (2011). Molecular dynamics simulation of heat transfer through interface between rough walls. *J. Eng. Thermophys-rus.* 32 (09), 1449–1453. (in Chinese).

Hong, K. T., Imadojemu, H., and Webb, R. L. (1994). Effects of oxidation and surface roughness on contact angle. *Exp. Ther. Fluid Sci.* 8, 279–285. doi:10.1016/0894-1777(94)90058-2

Kim, B. H., Beskok, A., and Cagin, T. (2008). Molecular dynamics simulations of thermal resistance at the liquid-solid interface. *J. Chem. Phys.* 129 (17), 174701–174708. doi:10.1063/1.3001926

Li, H. Y., Wang, J., and Xia, G. D. (2022). Thermal transport through solid-liquid interface: effect of the interfacial coupling and nanostructured surfaces. *J. Therm. Sci.* 31 (4), 1167–1179. doi:10.1007/s11630-022-1629-2

Li, Q., and Liu, C. (2012). Molecular dynamics simulation of heat transfer with effects of fluid-lattice interactions. *Int. J. Heat. Mass Tran.* 55 (25-26), 8088–8092. doi:10.1016/j.ijheatmasstransfer.2012.08.045

Liu, F. R., Chen, Z. X., and Li, Y. H. (2024). Effects of columnar nanostructures with mixed wettability on explosive boiling heat transfer of nanoscale argon film over copper plate. *J. At. Mol. Phys.* 41 (3), 032001. (in Chinese). doi:10.19855/j.1000-0364.2024.032001

Liu, H. Q., Deng, W., Ding, P., and Zhao, J. (2021). Investigation of the effects of surface wettability and surface roughness on nanoscale boiling process using molecular dynamics simulation. *Nucl. Eng. Des.* 382, 111400. doi:10.1016/j.nucengdes.2021.111400

Liu, H. Q., Qin, X. Y., Ahmad, S., Tong, Q., and Zhao, J. (2019). Molecular dynamics study about the effects of random surface roughness on nanoscale boiling process. *Int. J. Heat. Mass Tran* 145, 118799. doi:10.1016/j.ijheatmasstransfer.2019.118799

Liu, M., Xu, W. H., Xu, K., and Wang, Z. L. (2020). Study on thermal transport at interface between graphene film and semiconductor. *J. China Univ. Petroleum Edition Nat. Sci.* 44 (6), 103–108. (in Chinese).

Qian, C., Wang, Y., He, H., Huo, F., Wei, N., and Zhang, S. (2018). Lower limit of interfacial thermal resistance across the interface between an imidazolium ionic liquid and solid surface. *J. Phys. Chem. C* 122, 22194–22200. doi:10.1021/acs.jpcc.8b06974

Qian, C. Y., Yu, B. B., Ye, Z. H., Shi, J. Y., and Chen, J. P. (2024). Molecular dynamics simulation of interfacial heat transfer characteristics of CO_2, R_{32} and CO_2/R_{32} binary zeotropic mixture on a smooth substrate. *Int. J. Refrig* 157, 186–198. doi:10.1016/j.ijrefrig.2023.10.020

Song, F. H., Ma, J. M., Ye, Y. R., Wang, G., Fan, J., Chen, R., et al. (2025). Adsorption and energy storage characteristics of ionic liquids in porous zeolite-templated carbon materials. *Int. J. Heat. Mass Tran* 236, 126297. doi:10.1016/j.ijheatmasstransfer.2024.126297

Song, F. H., Niu, H., Fan, J., Chen, Q., Wang, G., and Liu, L. (2020). Molecular dynamics study on the coalescence and break-up behaviors of ionic droplets under DC electric field. *J. Mol. Liq.* 312, 113195. doi:10.1016/j.molliq.2020.113195

Song, F. H., Wang, F. K., Ma, J. M., Xue, J., and Fan, J. (2023). Microstructure of ionic liquids mixed with water on the charged graphene surface: a coarse-grained molecular dynamics simulation study. *J. Mol. Liq.* 391, 123253. doi:10.1016/j.molliq.2023.123253

Song, F. H., Xue, J. Y., Ma, B., Fan, J., Wang, Y. C., and Jiang, Y. H. (2022b). Wetting and electro-wetting behaviors of [Bmim] [Bf4] ionic liquid droplet on lyophobic and lyophilic solid substrates. *J. Mol. Liq.* 347, 118405. doi:10.1016/j.molliq.2021.118405

Song, L., Zhang, Y., Zhan, J., An, Y., Yang, W., Tan, J., et al. (2022a). Interfacial thermal resistance in polymer composites: a molecular dynamic perspective. *Mol. Simulat.* 48 (10), 902–925. doi:10.1080/08927022.2022.2071874

Su, D. D., Li, X. B., Zhang, H. N., and Li, F. C. (2024). Molecular dynamics simulation of interfacial heat transfer behavior during the boiling of low-boiling-point organic fluid. *Int. J. Heat. Mass Tran.* 220, 124962. doi:10.1016/j.ijheatmasstransfer.2023.124962

Sun, H., Liu, Z., Xin, G., Xin, Q., Zhang, J., Cao, B. Y., et al. (2020). Thermal and flow characterization in nanochannels with tunable surface wettability: a comprehensive molecular dynamics study. *Numer. Heat. Tr. A-Appl* 78 (6), 231–251. doi:10.1080/10407782.2020.1788849

Sun, Z. P., Zhang, D. L., Qi, Z. J., Wang, Q., Sun, X., Liang, K., et al. (2024). Insight into interfacial heat transfer of β-Ga_2O_3/diamond heterostructures via the machine learning potential. *ACS Appl. Mater. Interfaces* 16 (24), 31666–31676. doi:10.1021/acsami.3c19588

Tang, X. Y., Zeng, L., Zeng, Z. Y., and Feng, G. (2021). Molecular dynamics simulation of heat transfer through solid-liquid interface in ionic-liquid-based supercapacitors. *Sci. Sin. Chim.* 51, 1442–1449. doi:10.1360/ssc-2021-0094

Warzoha, R. J., Wilson, A. A., Donovan, B. F., Donmezer, N., Giri, A., Hopkins, P. E., et al. (2021). Applications and impacts of nanoscale thermal transport in electronics packaging. *J. Electron Packag.* 143 (2), 020804. doi:10.1115/1.4049293

Wu, N. N., Zeng, L. C., Fu, T., Wang, Z., and Lu, C. (2020). Molecular dynamics study of rapid boiling of thin liquid water film on smooth copper surface under different wettability conditions. *Int. J. Heat. Mass Tran* 147, 118905. doi:10.1016/j.ijheatmasstransfer.2019.118905

Yang, G., and Cao, B. Y. (2024). On the modelling of thermal boundary resistance in semiconductor heterostructures. *J. Eng. Thermophys-rus.* 45 (04), 1132–1138. (in Chinese).

Yin, X. Y., Hu, C. Z., Bai, M. L., and Lv, J. (2019a). Effects of depositional nanoparticle wettability on explosive boiling heat transfer: a molecular dynamics study. *Int. Commun. Heat. Mass* 109 (C), 104390. doi:10.1016/j.icheatmasstransfer.2019.104390

Yin, X. Y., Hu, C. Z., Bai, M. L., and Lv, J. (2019b). Effects of depositional nanoparticle wettability on explosive boiling heat transfer: a molecular dynamics study. *Int. Commun. Heat. Mass* 109, 104390. doi:10.1016/j.icheatmasstransfer.2019.104390

Zhang, S. Z., Chen, Z. X., Liu, F. R., Pang, R. Y., and Wang, Q. (2022). Molecular dynamics simulation of liquid boiling on nanostructured surfaces. *Chem. Ind. Eng. Pro.* 41 (5), 2311–2321. doi:10.16085/i.issn.1000-6613.2021-1175

Zhou, S. J., Qing, S., Zhang, X. H., Huang, H. M., and Hou, M. L. (2024). Molecular dynamics simulations of thermal transport of carbon nanotube interfaces. *Energies* 17 (6), 1506. doi:10.3390/en17061506